

Cygnus OB2 – a young globular cluster in the Milky Way

J. Knödlseider

INTEGRAL Science Data Centre, Chemin d'Ecogia 16, CH-1290 Versoix, Switzerland
Centre d'Etude Spatiale des Rayonnements, CNRS/UPS, B.P. 4346, F-31028 Toulouse Cedex 4, France

Received 22 March 2000; accepted

Abstract. The morphology and stellar content of the Cygnus OB2 association has been determined using 2MASS infrared observations in the J , H , and K bands. The analysis reveals a spherically symmetric association of $\sim 2^\circ$ in diameter with a half light radius of $13'$, corresponding to $R_h = 6.4$ pc at an assumed distance of 1.7 kpc. The interstellar extinction for member stars ranges from $A_V \approx 5^m$ to 20^m , which led to a considerable underestimation of the association size and richness in former optical studies. From the infrared colour-magnitude diagram, the number of OB member stars is estimated to 2600 ± 400 , while the number of O stars amounts to 120 ± 20 . This is the largest number of O stars ever found in a galactic massive star association. The slope of the initial mass function has been determined from the colour-magnitude diagram to $\Gamma = -1.6 \pm 0.1$. The total mass of Cyg OB2 is estimated to $(4 - 10) \times 10^4 M_\odot$, where the primary uncertainty comes from the unknown lower mass cut-off. Using the radial density profile of the association, the central mass density is determined to $\rho_0 = 40 - 150 M_\odot \text{pc}^{-3}$.

Considering the mass, density, and size of Cyg OB2 it seems untenable to classify this object still as OB association. Cygnus OB2 more closely resembles a young globular cluster like those observed in the Large Magellanic Cloud or in extragalactic star forming regions. It is therefore suggested to re-classify Cygnus OB2 as young globular cluster – an idea which goes back to Reddish et al. (1966). Cygnus OB2 would then be the first object of this class in the Milky Way.

Key words: Stars: early type – extinction – globular clusters – open clusters and associations: Cyg OB2 – Galaxy: stellar content

1. Introduction

The study of galactic OB associations provides the key to a number of astrophysical questions, such as the star for-

mation process and efficiency, the interaction of massive stars with the interstellar medium, the characterisation of the initial mass function at the high-mass end, the study of stellar nucleosynthesis, chemical evolution, and galactic recycling processes, and the evolution of binary systems. The Cygnus OB2 association is a particularly good region to address such questions, since it is extremely rich (e.g. Reddish et al. 1966, hereafter RLP), and contains some of the most luminous stars known in our Galaxy (e.g. Torres-Dodgen et al. 1991).

The most comprehensive study of the size and shape of Cyg OB2 has been performed by RLP who inferred an elliptical shape with major and minor axes of $48'$ and $28'$, respectively (see also Fig. 5). They estimate more than 3000 members of which at least 300 are of OB spectral type, resulting in a total stellar mass between $(0.6 - 2.7) \times 10^4 M_\odot$. For their analysis, RLP performed star counts on the blue and red plates of the Digitized Sky Survey (DSS), reaching limiting magnitudes around 20^m . Although this limit assures a reasonable complete census for unobscured associations, the extreme reddening in and around Cyg OB2 hampers the detection of even OB stars. With an estimated distance of 1.7 kpc (e.g. Massey & Thompson 1991) Cyg OB2 is located behind the Great Cygnus Rift, causing visual extinction A_V from 4^m to at least 10^m . A number of observations suggest that Cyg OB2 could indeed be larger than the RLP estimate, and that the observed morphology is rather an artifact of the particular extinction pattern in the field. The association boundary determined by RLP fits suspiciously well in a region of low CO column density (cf. Fig. 1) and low visual extinction (Dickel & Wendker 1978), indicating that the visual star densities are probably biased by the extinction pattern. There is a considerable number of early-type stars in the obscured area south and south-east of Cyg OB2 that are estimated to lie at the same distance as Cyg OB2, and that could indeed be bright member stars of the association. Examples are the Wolf-Rayet stars WR 145 and WR 146 (Niemela et al. 1998), the potential Luminous Blue Variable star G79.29+0.46 (Higgs et al. 1994), the massive binary system MWC 349 (Cohen et al. 1985), or

Send offprint requests to: Jürgen Knödlseider

Correspondence to: knodlseider@cesr.fr

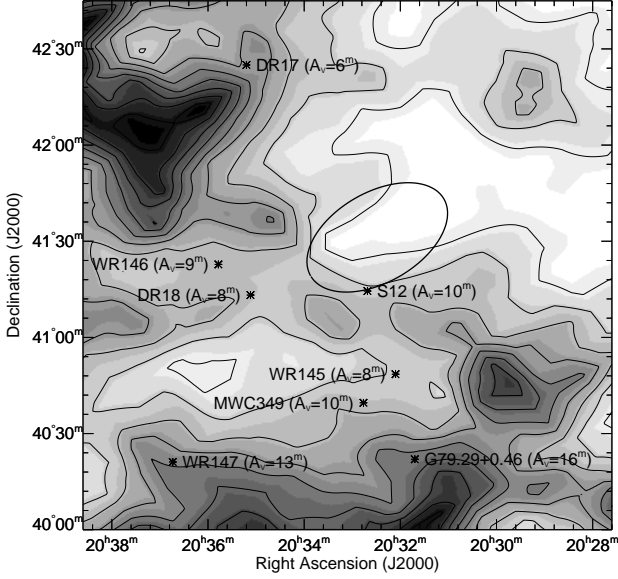


Fig. 1. Velocity integrated (-10 to 20 km s^{-1}) CO intensity map of the region around Cyg OB2 (from Leung & Thaddeus 1992). The ellipsoid indicates the size of Cyg OB2 as determined by RLP. Massive stars that may be associated to Cyg OB2 but lying outside the classical Cyg OB2 boundary of RLP are indicated by asterisks. Visual extinction estimates are quoted in parentheses.

the recently discovered group of massive stars around the H II region DR 18 (Comerón & Torra 1999).

The availability of the *Two Micron All Sky Survey* (2MASS) provides now an excellent opportunity to re-address the question on the morphology and stellar content of Cyg OB2. This survey covers the infrared bands J , H , and K which have proven to be an excellent tool for unveiling embedded star clusters due to the reduced impact of dust extinction at longer wavelengths. In the following I will use these data to determine the morphology and stellar content of Cyg OB2. It will turn out that the association is much larger and much richer than previously thought, making it the most massive young stellar association known in our Galaxy.

2. Sample selection and colour-magnitude diagrams

The analysis presented in this work is based on the second incremental release of the 2MASS point source catalogue (PSC) that contains positional and photometric data for 162 million objects in the J , H , and K bands. For the investigation of Cyg OB2, all stars within a square field of $2^\circ 45'$ in size, centred on $\alpha = 20^{\text{h}}33^{\text{m}}6^{\text{s}}$ and $\delta = +41^\circ 22.5'$ (J2000)¹ have been extracted from the catalogue, resulting in a total of 203318 selected objects. Differential star count

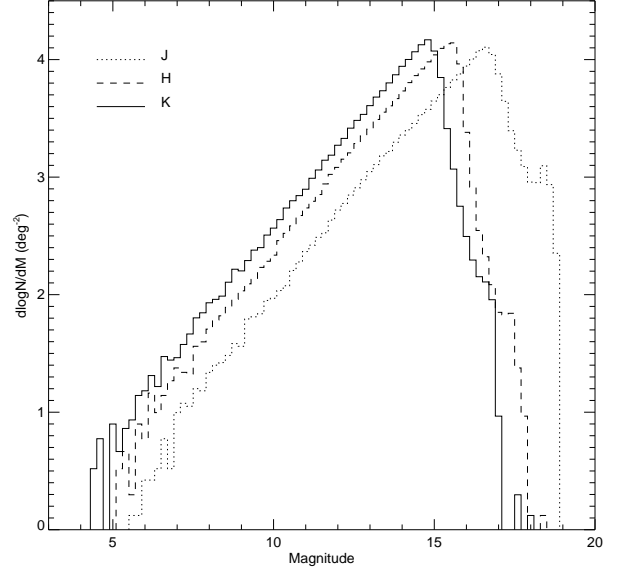


Fig. 2. Differential J , H , and K PSC star counts for a square field of $2^\circ 45'$ in size, centred on $\alpha = 20^{\text{h}}33^{\text{m}}6^{\text{s}}$ and $\delta = +41^\circ 22'30''$.

distributions for these stars in the 3 photometric bands are shown in Fig. 2. The positions of the turn-over in these distributions suggest that the selected sample is complete to magnitudes of 16.6, 15.5, and 14.8 in the J , H , and K bands, respectively. This is 0.5-0.8 magnitudes fainter than the nominal completeness limits of the PSC, as expected for less crowded areas in the galactic plane (Cutri et al. 2000). However, the limits have to be understood as an average for the investigated field, and enhanced crowding towards the centre of Cyg OB2 may lower the actual completeness magnitude for the association.

Colour-magnitude diagrams (CMDs) of the selected stars are presented in Fig. 3 as grey-scale plots, which have been obtained by counting the number of stars within pixels of 0.1 magnitudes in $J-K$ and K . For illustration, the sample has been divided into two distinct subsets:

- the *Cyg OB2 sample*, containing all stars within a circular region of 1.05° in radius, centred on $\alpha = 20^{\text{h}}33^{\text{m}}10^{\text{s}}$ and $\delta = +41^\circ 12'$
- the *field star sample*, containing all remaining stars outside the circular region.

The choice of the separation was motivated by the location and size of the Cyg OB2 association (cf. Sect. 4). Geometrically, the Cyg OB2 sample covers a field of 3.46 degrees squared while the field star sample covers 4.10 degrees squared. The number of stars in the CMDs is 100754 for the Cyg OB2 and 102167 for the field stars sample; 397 stars lie outside the plotted range. Normalising the number of stars in the field star sample to the geometrical area of the Cyg OB2 sample and subtraction from the Cyg OB2 sample results in an excess of 14420

¹ All coordinates given in this paper are for the epoch J2000.

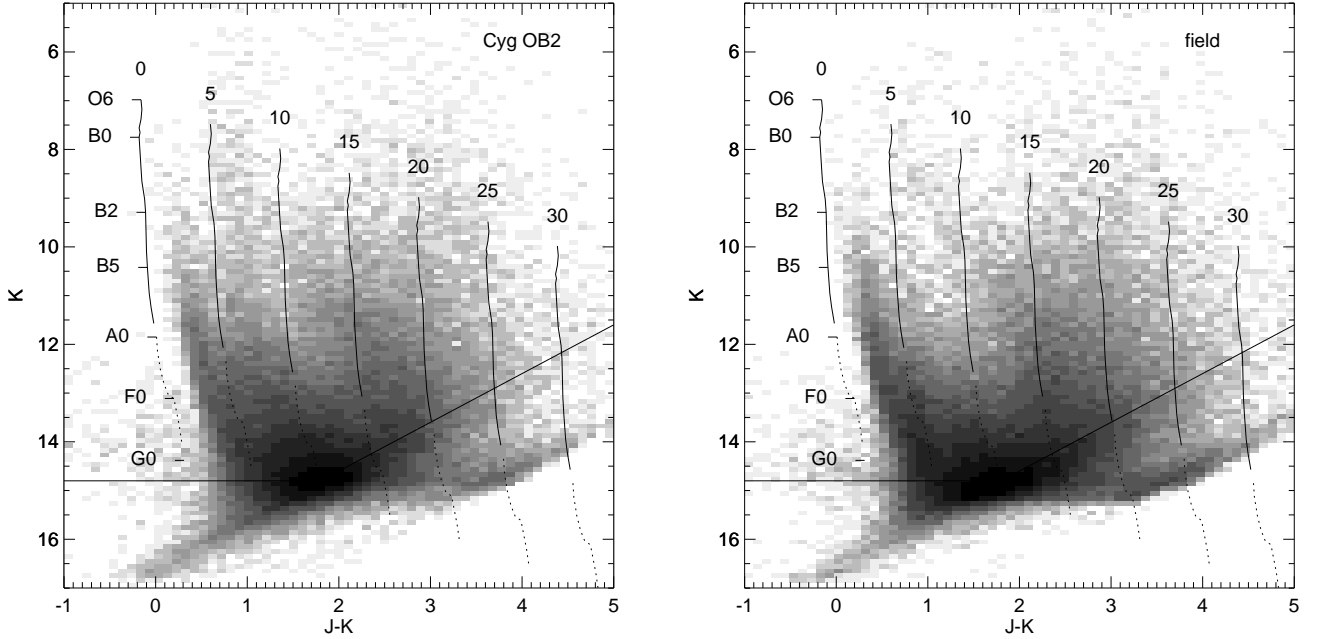


Fig. 3. Colour magnitude diagram for the Cyg OB2 region (left) and the field around Cyg OB2 (right). The estimated completeness limit is indicated as solid line. The unreddened main sequence for a distance modulus of 11.2 is shown as solid curve for OB stars and as dotted curve for A and F stars. Reddened main sequences are also shown for $A_V = 5$ to 30 in steps of 5 magnitudes.

stars within the association field. The CMD of these excess stars is shown in Fig. 4. This figure has been obtained by subtracting the field star CMD, multiplied by 0.85 to account for the different geometrical areas, from the Cyg OB2 sample CMD. To reduce statistical fluctuations the resulting CMD was smoothed with a boxcar average of 0.3 magnitudes in $J - K$ and K .

Figure 4 clearly illustrates the wide spread of visual extinctions in Cyg OB2, covering the range from $A_V \approx 5$ to 20 magnitudes. Between $A_V \approx 5 - 10$ magnitudes, a clear main sequence distribution is visible which spatially coincides with regions of low visual obscuration, as depicted by the light areas in the CO map (cf. Fig. 1). Stars more heavily reddened are related to regions of higher CO column density, located in particular south of the classical Cyg OB2 boundaries.

In the CMDs the PSC sample completeness limits manifest as a colour dependent K magnitude limit. For $J - K < 1.8$, the K magnitude limit of 14.8 is driving the sample completeness, while for $J - K > 1.8$ the J magnitude limit of 16.6 becomes dominant, resulting in a colour dependent completeness limit of $K = 16.6 - (J - K)$. The resulting limit is shown in Figs. 3 and 4 as solid line. For illustration, the unreddened main sequence for O to F type stars with a distance modulus of 11.2, as suggested by Massey & Thompson (1991) for Cyg OB2, is also shown (see Appendix A for a reference of the photometric calibrations). Reddened main sequences are also

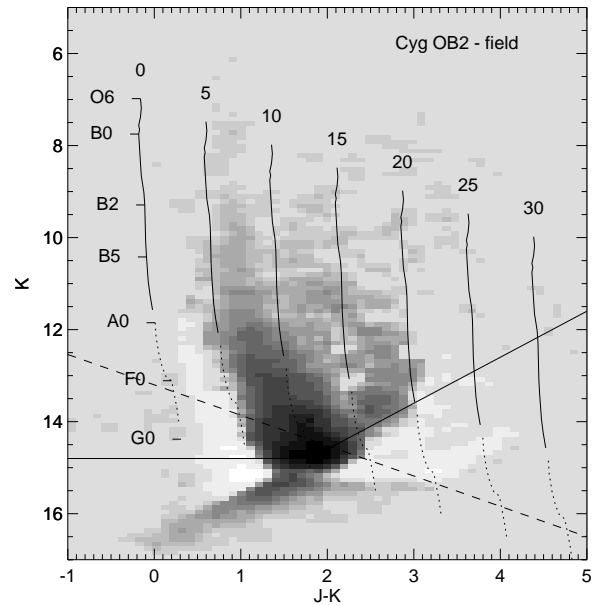


Fig. 4. CMD of the Cyg OB2 association. The dashed line indicates the colour dependent K magnitude selection applied to extract the stellar density distribution, limiting the sample to main sequence stars of spectral type F3V and earlier.

shown for $A_V = 5$ to 30 in steps of 5 magnitudes, assum-

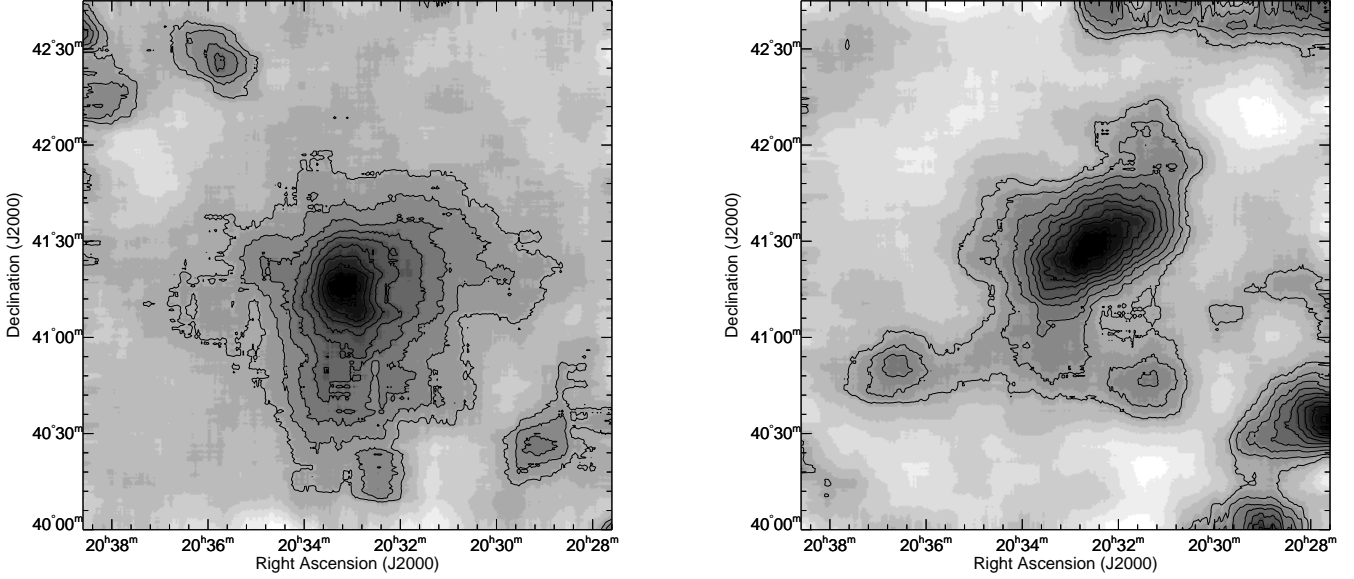


Fig. 5. Stellar density distributions derived from the 2MASS PSC catalogue (left) and DSS red plates (right). Dark regions correspond to high densities. Isodensity contours are superimposed, starting above the background stellar density in 10% steps with respect to maximum density. The stellar densities were smoothed with a boxcar average of $15'$ in order to emphasise the morphology of the association.

ing $A_V/A_K = 10$ and a reddening slope of $A_K/E(J - K)$ of 0.66 (Rieke & Lebofsky 1985).

Comparison of the reddened main sequences with the completeness limit suggests that the PSC is complete for OB stars in Cyg OB2 up to visual extinctions of $A_V \approx 20$ magnitudes. This is comparable to the maximum reddening found for the association stars (cf. Fig. 4), hence the OB stars sample in the PSC should be complete.

3. Morphology from star counts

To study the morphology of the Cyg OB2 association, the stellar density distribution of the field has been determined by binning the PSC stars in pixels of size $30'' \times 30''$. Only stars with K magnitude brighter than $13.2 + 0.66 \times (J - K)$ have been selected in order to minimise any bias through variable extinction, and to maximise at the same time the number of stars in the stellar density distribution. This selection is equivalent to choosing stars intrinsically brighter than $M_K \leq 2.2^m$ at the distance of Cyg OB2, corresponding to main sequence stars of spectral type F3V and earlier (cf. Appendix A). A comparison to the completeness limit in Fig. 4 shows that stars later than spectral type B9 and suffering from visual extinction in excess of $A_V \approx 12^m$ could be missed in the sample, but the CMD of Cyg OB2 suggests that only few association stars show these properties. Hence, the stellar density distribution should be relatively unaffected by absorption.

The presence of several bright stars in the field results in a couple of blind areas in the PSC where no in-

formation is available. These blind areas were filled by estimating their stellar densities from adjacent fields. A small ($\sim 10\%$) gradient in the field star density distribution has been removed by subtracting a 2-dimensional linear function that was estimated by fitting a lower envelope to the data. The resulting stellar density distribution is shown in the left panel of Fig. 5. For display, the distribution has been smoothed with a boxcar average of $15'$ to reduce statistical density fluctuations and to emphasise the global morphology of the association. Still, most of the fine structure in the image is probably of statistical nature and should be interpreted with care.

The image reveals a rather regular and almost circular stellar density profile for Cyg OB2 with a pronounced maximum at $\alpha = 20^h33^m10^s$ and $\delta = +41^\circ15.7'$. The maximum is slightly offset from the centre, which is determined to $\alpha = 20^h33^m10^s$ and $\delta = +41^\circ12'$ (see Sect. 4). Star counts in concentric radial annuli around the centre show that 50% of the members are located within a radius of $21'$, and 90% within a radius of $45'$ around the centre. The association merges with the field stars at a radius of $\sim 1^\circ$. Assuming a total diameter of 2° results in a physical diameter of 60 pc at a distance of 1.7 kpc.

A slight density enhancement at $\alpha = 20^h32^m12^s$ and $\delta = +40^\circ21'$ at the southern edge of Cyg OB2 possibly indicates some substructure in the association. The stars in this area show $J - K$ colours $> 2^m$, and are compatible with heavily reddened ($A_V > 12^m$) main sequence objects. The feature coincides spatially with the H II region DR 15 which has been identified as a nursery of embedded B stars (Odenwald et al. 1990). However, the distance of DR 15 is

quite uncertain (1–4.2 kpc; Wendker et al. 1991), making the physical association to Cyg OB2 highly speculative.

Two other features of localised stellar density enhancements are visible in Fig. 5. At $\alpha = 20^{\text{h}}35^{\text{m}}30^{\text{s}}$ and $\delta = +42^{\circ}25'$ a group of red ($J - K > 2^{\text{m}}$) stars coincide spatially with the extended H II region DR 17 (Wendker et al. 1991). Comparison with the CO map (cf. Fig. 1) suggests that also this feature could be an embedded star nursery, but its angular separation and estimated distance of 800 pc - 1.5 kpc (Odenwald & Schwartz 1993) make a physical relation to Cyg OB2 highly improbable. Another group of stars is found at $\alpha = 20^{\text{h}}29^{\text{m}}5^{\text{s}}$ and $\delta = +40^{\circ}25'$ which spans a wide range of colours, and which does not coincide with any known H II region or stellar cluster. The angular separation from Cyg OB2 suggests that this group is also not related to the association.

The morphology of Cyg OB2 as derived from the 2MASS catalogue is quite different to that inferred by RLP from DSS plates. While RLP found an elliptically shaped association of 29×17 pc in size, the PSC analysis presented in this work suggests a spherical association of 60 pc in diameter. To investigate the origin of this discrepancy, the stellar density distribution around Cyg OB2 has also been derived from the DSS red plates, reproducing Fig. 23 of RLP. The result of this analysis is shown in the right panel of Fig. 5, again smoothed by a boxcar average of $15'$ to enhance the morphology of the association. Indeed, the 2MASS and the DSS stellar density distributions are markedly different. Comparison with the matter distribution in the region (cf. Fig. 1) clearly shows that the morphology of the DSS density distribution is largely influenced by the absorption pattern. The elliptical shape of Cyg OB2 in the DSS data is produced by an elongated region of rather low extinction that is enclosed by two dust lanes running from south-east to north-west. Several local maxima that appear like extensions from the Cyg OB2 association are simply areas of reduced absorption, where the number of background stars is locally enhanced. A massive system of molecular clouds below $\delta = +40^{\circ}30'$ provides an efficient barrier for visible light, pushing the apparent centroid of Cyg OB2 towards the north. Hence DSS star counts are apparently not very suitable for the determination of the morphology of Cyg OB2. In contrast, a comparison with Fig. 1, and the above discussion of the completeness of the PSC sample, suggest that the 2MASS stellar density distribution is basically unaffected by absorption, hence it reveals indeed the true morphology of Cygnus OB2.

4. Size, mass, and stellar content

In order to determine the size, centre, and stellar content of Cyg OB2, radial star density profiles have been extracted from the 2MASS data by counting the number of stars intrinsically brighter than $M_K \leq 2.2^{\text{m}}$ in concentric radial annuli around an assumed centre, divided by the

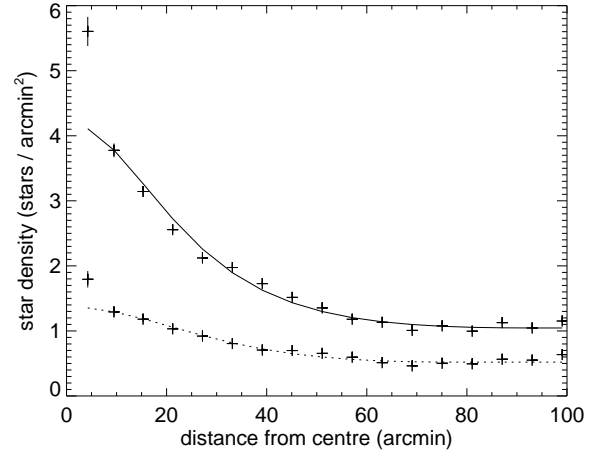


Fig. 6. Radial star density distribution for stars earlier than spectral type F3V (solid) and only OB type stars (dotted). The crosses present the observed stellar densities while the lines are fitted King profiles. An additional background star density was subtracted prior to the analysis in order to remove a small gradient ($\sim 10\%$) in the field star density. For the F3V sample, the zero point corresponds to a field star density of $3.1 \text{ stars arcmin}^{-2}$ while for the OB star sample the zero point amounts to $0.8 \text{ stars arcmin}^{-2}$.

annuli surface. Geometrical corrections have been applied for the outer annuli that partially fall outside the rectangular survey region. The profiles were fitted by a King law (King 1962)

$$f(r) = k \{ [1 + (r/r_c)^2]^{-1/2} - [1 + (r_t/r_c)^2]^{-1/2} \}^2 \quad (1)$$

on top of a constant to determine the core radius r_c , the tidal radius r_t , and the field star density. By searching the central position that minimises the radial extent of the profile the centre of Cyg OB2 has been determined to $\alpha = 20^{\text{h}}33^{\text{m}}10^{\text{s}}$ and $\delta = +41^{\circ}12'$. The corresponding density profile is shown in Fig. 6. The central stellar density reaches $4.5 \text{ stars arcmin}^{-2}$ above the field star density, and drops to 50% at a radius of $13'$, resulting in a half light radius of $R_h = 6.4 \text{ pc}$ at a distance of 1.7 kpc.

Best fitting King parameters for the profile are $r_c = 29' \pm 5'$ and $r_t = 93' \pm 20'$, leading to a concentration parameter $\log r_t/r_c$ of 0.5. The reduced χ^2 of the fit is only 10.9, indicating that the King law is not a very accurate description of the radial density profile. Indeed, there is no physical reason to believe that Cyg OB2 should follow a King profile. The basic aim of using King profiles was the estimation of the field star density, and comparison with Fig. 6 convinces that at least this goal was reached.

By integrating the radial profile after subtraction of the fitted field star density, the total number of association stars with $M_K \leq 2.2^{\text{m}}$ (corresponding to spectral types of F3V and earlier) amounts to 8600 ± 1300 . The error (as

all following error quotations) includes a possible systematic uncertainty from the field star subtraction. This systematic uncertainty was estimated by applying different methods for the extraction of the association stars, such as analysing star density profiles along constant Right Ascension or declination, estimating the field star density from a circular region around the association, or by performing the analysis without removing the gradient in the field star density distribution.

Selecting only K magnitudes brighter than $11.55 + 0.66 \times (J - K)$ limits the sample to stars intrinsically brighter than $M_K \leq 0.37^m$, corresponding roughly to spectral type B9V and earlier. Repeating the radial density profile analysis for this limited sample allows the determination of the total number of OB stars in Cyg OB2 to 2600 ± 400 . This number is at the upper end of the range quoted by RLP (300 - 3000), confirming their suggestion that many of the highly reddened stars in the DSS survey are indeed OB stars. Further, restricting $M_K \leq -3.55^m$, by requiring $K \leq 7.76 + 0.66 \times (J - K)$, selects only O stars from the PSC, resulting in a total number of 120 ± 20 objects. In their survey, Massey & Thompson (1991) find 40 O stars within a central field of 0.35 degrees squared of the Cyg OB2 association. Integrating over the same region in the 2MASS data gives 39 ± 6 O stars, demonstrating that the present analysis is in excellent agreement with the Massey & Thompson observations. Hence, the large number of O stars found in this analysis is mainly due to the large extent of the association, which previously was missed due to the high extinction in the area.

Taking an initial mass of $1.5 M_\odot$ for a F3V star (Schmidt-Kaler 1982), and assuming the slope Γ of the initial mass function (IMF)² to be comprised between -1.1 and -1.7 , the number of association stars converts into a total stellar mass of $(3 - 5) \times 10^4 M_\odot$ above $1.5 M_\odot$. Extrapolation of the IMF to lower masses using the prescription of Kroupa et al. (1993) results in a total association mass of $(4 - 10) \times 10^4 M_\odot$, where the boundaries correspond to a lower mass cut-off of 1.0 and $0.08 M_\odot$, respectively. Since the actual value of the mass cut-off in Cyg OB2 is unknown, the total association mass is uncertain to within the quoted limits. However, even at the lower mass limit, Cyg OB2 would be the most massive OB association known in the Galaxy, being comparable in mass to a small globular cluster.

From the radial density profile and the total mass estimates, the central mass density of Cyg OB2 can be estimated. Assuming a total mass of $4 \times 10^4 M_\odot$ results in a mass density of $\rho_0 = 40 - 60 M_\odot \text{ pc}^{-3}$, where the lower value comes from the extrapolation of the best fitting King profile into the centre, and the upper value comes from the observed central stellar density. Correspondingly, the central mass density estimate for a total mass of 1×10^5

M_\odot amounts to $\rho_0 = 100 - 150 M_\odot \text{ pc}^{-3}$. As before, the distance to Cyg OB2 has been assumed to 1.7 kpc.

5. Initial mass function

To derive the mass spectrum of Cyg OB2, sub-samples of the PSC data containing all member stars within a given interval $[M_K^{\text{low}}, M_K^{\text{up}}]$ of intrinsic K magnitudes have been defined. Additionally, the K band extinctions A_K were restricted to the range $0 \leq A_K \leq 2$ that has been found to enclose the association members (cf. Sect. 2). To define the intrinsic K magnitude intervals, photometric cuts along the reddening lines have been applied using

$$\tilde{K}_{\text{low}} \geq K - DM - 0.66 \times (J - K) \geq \tilde{K}_{\text{up}} \quad (2)$$

where $M_K = 0.0037 + 1.036 \times \tilde{K}$. The extinction cut was realised using the relation

$$A_K \approx \frac{K + 0.057 - 17.835 \times (J - K) - DM}{1 - 17.835/0.66} \quad (3)$$

which is an approximation of the extinction at the distance of Cyg OB2 as function of the position in the CMD for $M_K \leq 2^m$ (see Appendix B for details about the derivation of these relations). In Eqs. (2) and (3), $DM = 11.2$ is the assumed distance modulus of Cyg OB2.

Using these equations, the $K, J - K$ plane has been divided into 7 areas of identical size which define 7 stellar sub-samples in the PSC data (cf. Fig. 7). The corresponding $[\tilde{K}_{\text{low}}, \tilde{K}_{\text{up}}]$ and $[M_K^{\text{low}}, M_K^{\text{up}}]$ intervals are summarised in Table 1. The $[M_K^{\text{low}}, M_K^{\text{up}}]$ intervals have then been converted into initial mass intervals using the mass-luminosity relation derived in Appendix A. The corresponding mass boundaries are quoted in the last two columns of Table 1.

Table 1. Selection parameters of the seven sub-samples.

\tilde{K}_{low}	\tilde{K}_{up}	M_K^{low}	M_K^{up}	$\log M^{\text{low}}$	$\log M^{\text{up}}$
2	1	2.08	1.04	0.196	0.407
1	0	1.04	0.00	0.407	0.613
0	-1	0.00	-1.03	0.613	0.826
-1	-2	-1.03	-2.07	0.826	1.048
-2	-3	-2.07	-3.10	1.048	1.285
-3	-4	-3.10	-4.14	1.285	1.654
-4	-5	-4.14	-5.18	1.654	2.211

Two methods have been employed to extract the IMF from the PSC data. First, radial density profiles have been derived for the 7 sub-samples which were then fitted by King profiles in order to estimate the field star density in each of the samples. The field star density estimate was then subtracted from the radial density profile, and integration over the residual profile provided an estimate of the number of member stars in the sub-sample. Note that

² The Salpeter IMF has a slope of $\Gamma = -1.35$ in this prescription.

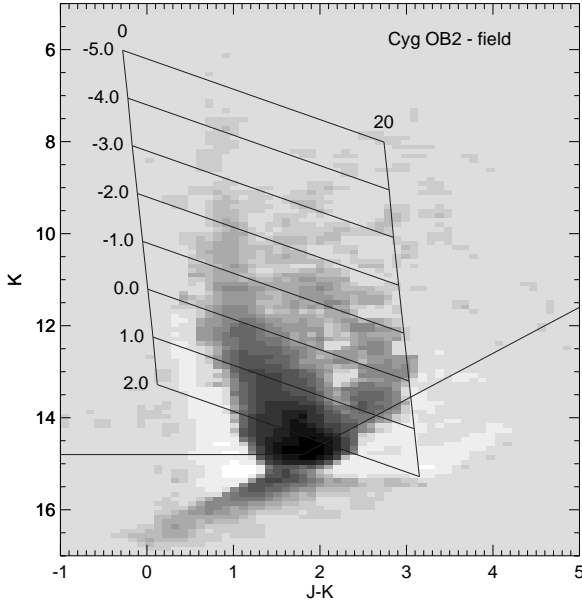


Fig. 7. CMD of the Cyg OB2 association with photometric cuts superimposed that have been applied to determine the IMF. The limits \tilde{K} of Eq. (2) are quoted at the left edge of the selected areas.

this method properly accounts for possible variations in the size of the association for different intrinsic magnitude intervals, which could result from mass segregation. However, the analysis revealed similar radial extents for all 7 sub-samples, indicating that no mass segregation has taken place in Cyg OB2. The second method consisted simply in integrating the number of stars in the field star subtracted CMD in the 7 areas indicated in Fig. 7. Here, the field star density is estimated from the area beyond 1.05° from the association centre, as discussed in Sect. 2. Note that in this case the gradient in the field stars density distribution has not been removed.

The results of both analyses are summarised in Fig. 8. The points with error bars were derived using radial density profiles (i.e. the first method), while the results from integrating the CMD are shown as diamonds. Apparently, both methods lead to consistent IMFs. The data points are reasonably well fitted by a power law IMF of slope $\Gamma = -1.6 \pm 0.1$ for both methods. The slope is compatible with the Kroupa et al. (1993) analysis of the solar neighbourhood, but considerably steeper than $\Gamma = -1.0 \pm 0.1$ determined by Massey & Thompson (1991) for the central part of Cyg OB2. Note, however, that photometric mass determinations, as performed in this work, are less reliable than a spectroscopic study, as done by Massey & Thompson (1991), and a change in the employed mass-luminosity relation could easily flatten the IMF. On the other hand, the Massey & Thompson (1991) analysis did not extend to such low masses as the present

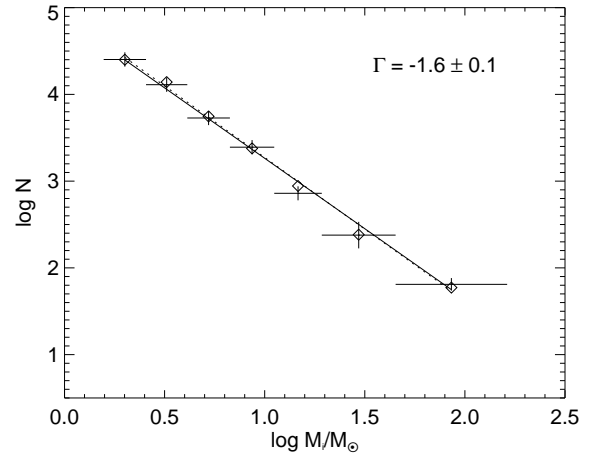


Fig. 8. IMF for Cygnus OB2. The solid line presents the best fitting power law to the points derived from radial density profiles (crosses) while the dotted line is the best fitting power law to the CMD integrated data (diamonds).

analysis does, and the flat slope they determined could also reflect an incompleteness in the lower mass domain.

Finally, Fig. 7 suggests that the lowest mass bin could be subject to incompleteness since the integration region extends below the completeness limit. In particular, the completeness limit for the central part of Cyg OB2 may lie at even smaller magnitudes due to enhanced crowding, making $\Gamma = -1.6$ formally to a lower limit for the slope of the IMF. Nevertheless, the lowest mass bins in Fig. 8 fall not particularly below the IMF extrapolation from the higher masses, indicating that there are probably not many member stars which are missed. The number of 8600 ± 1300 members earlier than spectral type F3V, derived in Sect. 4, is therefore probably a solid value.

6. Conclusions

The analysis of 2MASS data from the Cygnus region has revealed that Cygnus OB2 is considerably larger and more massive than previously thought. Previous surveys in the visible wavelength range, such as the extensive work of RLP, were substantially biased by the local extinction pattern in the field, which is caused by a foreground molecular cloud structure, known as the Great Cygnus Rift. The infrared data reveal now a spherically shaped association, with stellar extinctions reaching $A_V \approx 20^m$ in the southern part of the field. Several highly reddened early-type objects that formerly were situated outside the association boundary are now lying within the association, indicating that they possibly are members of Cyg OB2. Examples are the massive binary system MWC349 (Cohen et al. 1985), the potential Luminous Blue Variable star G79.29+0.46 (Higgs et al. 1994), the Wolf-Rayet stars WR 145 and WR 146 (Niemela et al. 1998), and the recently discov-

ered group of massive stars around the H II region DR 18 (Comerón & Torra 1999). Deep spectroscopic surveys of the stars in the highly obscured regions should help to consolidate the stellar population of Cyg OB2, and will improve our knowledge about the evolutionary state of the association.

Table 2. Summary of Cyg OB2 properties (radial dimensions and the central mass density have been calculated for an assumed distance of 1.7 kpc).

Centre (J2000)	$\alpha = 20^{\text{h}}33^{\text{m}}10^{\text{s}}, \delta = +41^{\circ}12'$
Diameter	$\sim 2^{\circ}$ (~ 60 pc)
Half light radius R_h	$13'$ (6.4 pc)
Core radius r_c	$29' \pm 5'$ (14 ± 2 pc)
Tidal radius r_t	$93' \pm 20'$ (46 ± 10 pc)
Members earlier F3V	8600 ± 1300
OB star members	2600 ± 400
O star members	120 ± 20
Total stellar mass	$(4 - 10) \times 10^4 M_{\odot}$
Central mass density ρ_0	$40 - 150 M_{\odot} \text{ pc}^{-3}$
IMF slope Γ	-1.6 ± 0.1

RLP already recognised from their analysis that Cyg OB2 is unusually massive and compact, and hence suggested that it should be regarded as a new globular cluster of stars, similar to the blue globular clusters discovered by Hodge (1961) in the Large Magellanic Cloud (LMC). Indeed, the comparison of the association parameters, summarised in Table 2, to typical parameters for galactic OB associations, young open clusters, and globular clusters leads inevitably to this conclusion. For an OB association, Cyg OB2 is simply too compact. The typical mass density of OB associations is well below $0.1 M_{\odot} \text{ pc}^{-3}$ (Blaauw 1964) and the mean size amounts to 137 pc (Garmany 1994). Cyg OB2, however, shows an average mass density of $5 - 12 M_{\odot} \text{ pc}^{-3}$ within the inner 10 pc and a diameter of only 60 pc. Hence, in contrast to classical OB association, Cyg OB2 should be a gravitationally bound system (Blaauw 1964). Garmany & Stencel (1992) suggest that Cyg OB2 might be the nucleus of an OB association, hence it could be considered as an open cluster. However, for an open cluster (as well as for an OB association) Cyg OB2 is by far too massive. Typical masses for open clusters are at most $10^3 M_{\odot}$ and do not exceed $10^4 M_{\odot}$ (Bruch & Sanders 1983) while the total mass of Cyg OB2 amounts to $4 - 10 \times 10^4 M_{\odot}$. Such a high mass is more representative for a small globular cluster.

In particular, the parameters of Cyg OB2 (as listed in Table 2) correspond fairly well to the typical parameters derived for young globular clusters in the LMC (e.g. Elson et al. 1987; Fischer et al. 1992). They have masses $\sim 10^4 - 10^5 M_{\odot}$, central densities $\sim 10^2 M_{\odot} \text{ pc}^{-3}$, and extend to radii ~ 80 pc. Little or no mass segregation is observed in these objects and they show only a small age

spread (Elson et al. 1989). The same is true for Cyg OB2. The determination of radial profiles for different intrinsic luminosities did not reveal any mass segregation, and the analysis of a sub-sample of massive stars in Cyg OB2 by Massey & Thompson (1991) did not suggest a considerable age spread. Thus I believe it is reasonable to conclude that Cygnus OB2 shows the same properties as the system of young globular clusters in the LMC – hence Cygnus OB2 should be considered as a member of this population.

Cyg OB2 is the first object of this class that has been identified within our own Galaxy. Young globular clusters (or young populous clusters as termed by Hodge (1961)) seem not to be rare objects. They were first identified in the LMC but are now also found using the *Hubble Space Telescope* in a variety of extragalactic star forming regions (Ho 1997). Although young globulars are often observed in association with starburst phenomena, they also appear to form in more quiescent environments, such as circumnuclear rings in relatively undisturbed galaxies (e.g. Maoz et al. 1996). It seems therefore plausible that such a system can also form in our own Galaxy, although the formation conditions are yet to be explored.

In a review about young globulars in the LMC, Freeman (1980) asked why these systems “form in the LMC and not in the Galaxy”? Apparently, they do also form in our Galaxy, but heavy obscuration through the interstellar gas and dust make them difficult to detect – or may leave them unrecognised. Infrared surveys may help to improve the detectability of such systems, although the sensitivity and confusion limits restrict such studies to within a few kpc. Alternatively, one may search for the fingerprints that these systems leave on the surrounding interstellar medium (ISM). An example is the thermal radio emission related to the ionisation of the ISM by the numerous massive stars. Indeed, the 120 O stars in Cyg OB2 produce a Lyman continuum flux of roughly 10^{51} photons s^{-1} , making it probably the most important source of ionisation in the Cygnus X complex. It has been suggested that the Cygnus X complex could be a large Strömgren sphere powered by Cyg OB2 (Landecker 1984 and references therein), hence the search for similar complexes in surveys of thermal radio emission could provide hints for further young globulars in the Galaxy.

Another tracer may come from the emerging field of gamma-ray line spectroscopy. The massive stars in Cyg OB2 are an important source of radioisotopes that are expelled through stellar winds and supernova explosions into the interstellar medium. These isotopes eventually emit monoenergetic gamma-ray photons that arise from nuclear de-excitations following the radioactive decay. An example is the 1.809 MeV gamma-ray line arising from the decay of radioactive ^{26}Al , an isotope with a lifetime of $\sim 10^6$ years (see Prantzos & Diehl 1996 for a review). Indeed, besides the central galactic radian, the Cygnus X region is the most intense source of 1.809 MeV photons known in the Galaxy, which can be well explained by ^{26}Al

production in massive stars within Cyg OB2 (Knödlseeder et al., in preparation). A more detailed study of the galactic plane in the 1.809 MeV gamma-ray line by the upcoming *INTEGRAL* mission (Vedrenne et al. 1999) could lead to the identification of further regions of high star forming activity, and hence provide a unique tool to unveil young globular clusters in our own Galaxy.

Acknowledgements. This publication makes use of data products from the Two Micron All Sky Survey, which is a joint project of the University of Massachusetts and the Infrared Processing and Analysis Center/California Institute of Technology, funded by the National Aeronautics and Space Administration and the National Science Foundation. The author wants to thank T. Dame for kindly providing the CO data of the Cygnus region. The author is supported by an external ESA fellowship.

Appendix A: Stellar calibrations

The analysis presented in this work makes use of calibrations between intrinsic K magnitudes and $J - K$ colours on the one side, and spectral types and initial masses on the other side. The employed calibrations, valid for luminosity class V, are summarised in Table A.1. The use of luminosity class V calibrations for all stars is justified by the young age of Cyg OB2 (Massey & Thompson 1991).

The relation between spectral type and absolute visual magnitudes M_V has been compiled from data published by Vacca et al. (1996) for O3V - B0.5V stars, Humphreys & McElroy (1984) for B1V - B3V stars, and Schmidt-Kaler (1982) for B5V - G0V stars. The intrinsic colour calibrations $(V - K)_0$ and $(J - K)_0$ were taken from Wegner (1994) for spectral types O6V - B9V and from Koornneef (1983) for later spectral types. The $(V - K)_0$ calibration of Wegner (1994) was extrapolated in the $M_V, (V - K)_0$ plane to spectral type O3V using the relation

$$(V - K)_0 = -0.296 + 0.114 \times M_V \quad (\text{A.1})$$

which has been obtained from a fit to the data for spectral types B2V and earlier. The same relation was also used to interpolate the $(V - K)_0$ calibration for some O subtypes that were not covered by the analysis of Wegner (1994).

Based on the M_V and $(V - K)_0$ calibrations, the intrinsic K magnitudes were derived using

$$M_K = M_V - (V - K)_0. \quad (\text{A.2})$$

To derive the mass-luminosity relation, the initial stellar mass to spectral type relation has been taken from Schaerer & de Koter (1997) for O and Schmidt-Kaler (1982) for later type stars. Using a fit in the $\log M, M_K$ plane, the following relation has been established

$$\log M = \begin{cases} 0.605 - 0.201M_K + 0.0055M_K^2 & M_K > -3.70 \\ -0.630 - 0.557M_K & \text{else} \end{cases} \quad (\text{A.3})$$

Appendix B: Photometric sample selection

For the photometric sample selection two constraints have been applied in the $K, J - K$ plane. First, all association stars with identical intrinsic magnitude M_K are collected along the reddening line. To understand the selection, recall that the apparent K magnitude of a Cyg OB2 member star is related to the intrinsic magnitude M_K , the extinction A_K , and the distance modulus DM via

$$K = M_K + DM + A_K. \quad (\text{B.1})$$

The extinction of a star can be estimated from the colour excess

$$E(J - K) = (J - K) - (J - K)_0 \quad (\text{B.2})$$

using

$$A_K = 0.66 \times E(J - K) \quad (\text{B.3})$$

(Rieke & Lebofsky 1985). Thus all member stars of identical intrinsic magnitude but different extinction lie in the $K, J - K$ CMD on a line of constant slope, given by

$$K = M_K - 0.66 \times (J - K)_0 + DM + 0.66 \times (J - K). \quad (\text{B.4})$$

Hence, selecting stars within a band

$$\tilde{K}_{\text{low}} \geq K - DM - 0.66 \times (J - K) \geq \tilde{K}_{\text{up}} \quad (\text{B.5})$$

results in a reddening independent selection of stars, where

$$\tilde{K} \equiv M_K - 0.66 \times (J - K)_0. \quad (\text{B.6})$$

The values of \tilde{K} are listed in column 6 of Table A.1. Fitting a linear relation to these data results in

$$M_K = 0.0037 + 1.036 \times \tilde{K}. \quad (\text{B.7})$$

Second, the K band extinction A_K of an association star can be estimated by calculating its displacement along the reddening line. To understand this, notice that for main sequence stars, M_K is a function of intrinsic colour $(J - K)_0$, which for massive stars can be roughly approximated by a linear function. From the calibration table (cf. Table A.1) the relation

$$M_K \approx -0.057 + 17.835 \times (J - K)_0 \quad (\text{B.8})$$

has been determined for $M_K < 2^m$. Using Eqs. (B.2) and (B.3) the relation can be rewritten as

$$M_K \approx -0.057 + 17.835 \times \left((J - K) - \frac{A_K}{0.66} \right). \quad (\text{B.9})$$

Replacing this approximation in Eq. (B.1) and solving for A_K result in an approximative relation between apparent magnitude and colour and extinction in the K band:

$$K \approx \frac{K + 0.057 - 17.835 \times (J - K) - DM}{1 - 17.835/0.66}. \quad (\text{B.10})$$

Table A.1. Stellar calibrations employed in this work (all data are for luminosity class V). \tilde{K} was calculated using the relation $\tilde{K} = M_K - 0.66 \times (J - K)_0$ (see Appendix B).

Sp. Type	M_V	$(V - K)_0$	M_K	$(J - K)_0$	\tilde{K}	$\log M$
O3	-5.78	-0.95	-4.83			2.08
O4	-5.55	-0.93	-4.62			1.93
O4.5	-5.44	-0.92	-4.52			
O5	-5.33	-0.90	-4.43			
O5.5	-5.22	-0.89	-4.33			1.78
O6	-5.11	-0.89	-4.22	-0.16	-4.11	
O6.5	-4.99	-0.86	-4.13			
O7	-4.88	-0.86	-4.02	-0.15	-3.92	1.60
O7.5	-4.77	-0.84	-3.93			
O8	-4.66	-0.84	-3.82	-0.16	-3.71	
O8.5	-4.55	-0.81	-3.74			
O9	-4.43	-0.79	-3.64	-0.18	-3.52	1.40
O9.5	-4.32	-0.77	-3.55	-0.17	-3.44	
B0	-4.21	-0.76	-3.45	-0.18	-3.33	1.30
B0.5	-3.51	-0.69	-2.82	-0.16	-2.71	1.25
B1	-3.20	-0.66	-2.54	-0.15	-2.44	
B1.5	-2.80	-0.62	-2.18	-0.12	-2.10	
B2	-2.50	-0.59	-1.91	-0.11	-1.84	
B3	-1.60	-0.49	-1.11	-0.10	-1.04	0.88
B5	-1.20	-0.42	-0.78	-0.09	-0.72	0.77
B7	-0.60	-0.35	-0.25	-0.07	-0.20	
B8	-0.25	-0.29	0.04	-0.05	0.07	0.58
B9	0.20	-0.17	0.37	-0.02	0.38	
A0	0.65	0.00	0.65	0.01	0.64	0.46
A1	1.00	0.06	0.94	0.02	0.93	
A2	1.30	0.13	1.17	0.04	1.14	
A3	1.50	0.20	1.30	0.05	1.27	
A5	1.95	0.35	1.60	0.09	1.54	0.30
A7	2.20	0.45	1.75	0.12	1.67	
A8	2.40	0.56	1.84	0.14	1.75	
F0	2.70	0.79	1.91	0.20	1.78	0.20
F5	3.50	1.01	2.49	0.26	2.32	0.15
F8	4.00	1.12	2.88	0.29	2.69	
G0	4.40	1.22	3.18	0.31	2.98	0.02

References

- Blaauw A. 1964, ARA&A 2, 213
Bruch A., Sanders W.L. 1983, A&A 121, 237
Comerón F., Torra J. 1999, A&A 349, 605
Cohen M., Biegging J.H., Dreher J.W., Welch W.J. 1985, ApJ 292, 249
Cutri R.M., Skrutskie M.F., Van Dyk S., et al. 2000, Explanatory Supplement to the 2MASS Second Incremental Data Release, <http://www.ipac.caltech.edu/2mass/releases/second/doc/explsup.html>
Dickel H.R., Wendker H.J. 1978, A&A 66, 289
Elson R.A.W., Fall S.M., Freeman C. 1987, ApJ 323, 54
Elson R.A.W., Fall S.M., Freeman C. 1989, ApJ 336, 734
Fischer P., Welch D.L., Cote P., et al. 1992, AJ 103, 857
Freeman K.C. 1980, in: Star Clusters, IAU Symp. No. 85, ed. James E. Hesser, p. 317
Garmany C.D. 1994, PASP 106, 25
Garmany C.D., Stencel R.E. 1992, A&AS 94, 211
Higgs L.A., Wendker H.J., Landecker T.L. 1994, A&A 291, 295
Ho L.C. 1997, RMAA 6, 5
Hodge P.W. 1961, ApJ 133, 413
Humphreys R.M., McElroy D.B. 1984, ApJ 284, 565
King I. 1962, AJ 67, 471
Koornneef J. 1983, A&A 128, 84
Kroupa P., Tout C. A., Gilmore G. 1993, MNRAS 262, 545
Landecker T.L. 1984, AJ 89, 95
Leung H.O., Thaddeus P. 1992, ApJS 81, 267
Maoz D., Barth A.J., Sternberg A., et al. 1996, AJ 111, 2248
Massey P., Thompson A.B. 1991, AJ 101, 1408
Niemela V.S., Shara M.M., Wallace D.J., et al. 1998, ApJ 115, 2047
Odenwald S.F., Schwartz P.R. 1993, ApJ 405, 706
Odenwald S.F., Cambell M.F., Shivanandan K., et al. 1990, AJ 99, 288
Prantzos N., Diehl R. 1996, Phys. Rep. 267, 1
Reddish V.C., Lawrence L.C., Pratt N.M., 1966, Publs. R. Obs. Edinburgh 5, 111 (RLP)
Rieke G.H., Lebofsky M.J., 1985, ApJ 288, 618

- Schaerer D., de Koter A. 1997, A&A 322, 598
 Schmidt-Kaler Th. 1982, Landolt-Börnstein Vol. 2
 Torres-Dodgen A.V., Tapia M., Carroll M. 1991, MNRAS 249,
 1
 Vacca W.D., Garmany C.D., Shull J.M. 1996, ApJ 460, 914
 Vedrenne G., Schönfelder V., Albernhe F., et al. 1999, Astro.
 Lett. and Communications 39, 325
 Wendker H.J., Higgs L.A., Landecker T.L. 1991, A&A 241, 551
 Wegner W. 1994, MNRAS 270, 229